Functional Mimicry of a Protein Hormone by a Peptide Agonist: The EPO Receptor Complex at 2.8 Å

Oded Livnah, Enrico A. Stura, Dana L. Johnson, Steven A. Middleton, Linda S. Mulcahy, Nicholas C. Wrighton, William J. Dower, Linda K. Jolliffe, Ian A. Wilson*

The functional mimicry of a protein by an unrelated small molecule has been a formidable challenge. Now, however, the biological activity of a 166-residue hematopoietic growth hormone, erythropoietin (EPO), with its class 1 cytokine receptor has been mimicked by a 20-residue cyclic peptide unrelated in sequence to the natural ligand. The crystal structure at 2.8 Å resolution of a complex of this agonist peptide with the extracellular domain of EPO receptor reveals that a peptide dimer induces an almost perfect twofold dimerization of the receptor. The dimer assembly differs from that of the human growth hormone (hGH) receptor complex and suggests that more than one mode of dimerization may be able to induce signal transduction and cell proliferation. The EPO receptor binding site, defined by peptide interaction, corresponds to the smaller functional epitope identified for hGH receptor. Similarly, the EPO mimetic peptide ligand can be considered as a minimal hormone, and suggests the design of nonpeptidic small molecule mimetics for EPO and other cytokines may indeed be achievable.

Erythropoietin (EPO) is the primary hormone that regulates the proliferation and differentiation of immature erythroid cells (*1*). In mammals, EPO is produced in fetal liver and adult kidney in response to hypoxia, and circulates in the bloodstream where it targets EPO receptor (EPOR) on committed progenitor cells in the bone marrow and other hematopoietic tissues (*1*). Recombinant human erythropoietin is widely used in the treatment of patients with anemia due to renal failure, cancer chemotherapy, and AZT treatment (*2*). The EPOR belongs to the cytokine receptor superfamily, which includes receptors for other hematopoietic growth factors, such as interleukins (IL) and colony-stimulating factors (CSF), as well as growth hormone (GH), prolactin, and ciliary neurotrophic factor (CNTF) (*3*). The structural architecture of this family of receptors consists of three modules: a ligand binding extracellular subunit, a single transmembrane region and a cytoplasmic domain. Bazan (*3*) has proposed that the extracellular portion of this receptor superfamily comprises two discrete domains (named here D1 and D2), each containing approximately 100 residues that fold into a sandwich consisting of seven antiparallel β strands with the topology of an immunoglobulin (Ig) constant domain. Members of the family share two characteristic motifs in their extracellular domains, namely, a pair of conserved disulfide bridges in the NH_2-terminal domain (D1), and a WSXWS box (*4*) in the COOH-terminal domain (D2). Oligomerization of one or more polypeptide chains is often essential for forming functional, high affinity receptor complexes (*5*). A homodimer complex is the active form of human growth hormone receptor (hGHR) (*6*, *7*), and a similar model has been suggested for granulocyte–colony-stimulating factor (G-CSF), prolactin, and EPORs (*5*, *8*). Dimerization of EPOR is proposed to lead to phosphorylation of its cytoplasmic domains by association with Janus kinase 2 (JAK2) to trigger the cascade of events that results in cell proliferation (*9*).

A family of disulfide-linked cyclic peptides that binds EPOR and functions both in vitro and in vivo as mimetics of EPO has been identified (*10*). A consensus sequence was determined (*10*) by screening a library of random peptide sequences displayed on filamentous phage against immobilized EPOR. EPO mimetic peptide 1 (EMP1) [GGTYSCHFGPLTWVCKPQGG] (*11*), a highly potent member of the family, is characterized by an intramolecular disulfide bridge, and contains several residues that appear frequently in the phage selection process and affect activity (*10*). Several lines of evidence suggest that the biological activity of EMP1 is mediated through interaction with EPOR (*10*). EMP1 competes

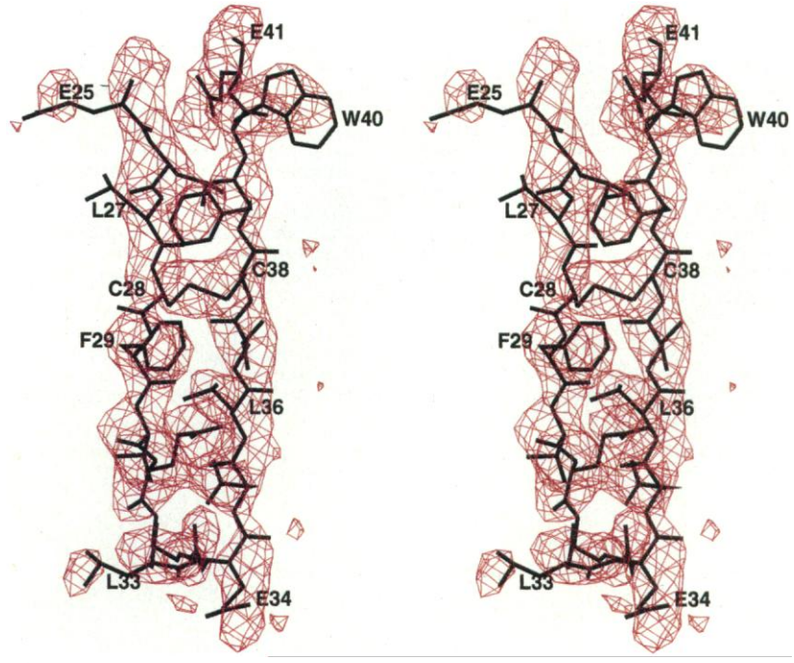

Fig. 1. Stereoview of the initial experimental solvent-flattened MIR electron density map at 25.0 to 3.1 Å resolution, contoured at 1.3 σ for residues 25 to 41 with superimposed coordinates from the final refined structure. This segment covers β strands A and B in D1 and shows one of the two characteristic disulfide bridges [Cys^{28}–Cys^{38}] in the first domain of the cytokine receptor superfamily.

O. Livnah, E. A. Stura, and I. A. Wilson are in the Department of Molecular Biology and at the Skaggs Institute of Chemical Biology, The Scripps Research Institute, 10666 North Torrey Pines Road, La Jolla, CA 92037, USA. D. L. Johnson, S. A. Middleton, L. S. Mulcahy, and L. K. Jolliffe are at the R. W. Johnson Pharmaceutical Research Institute, Drug Discovery Research, 1000 Route 202, Box 300, Raritan, NJ 08869, USA. N. C. Wrighton and W. J. Dower are at Affymax Research Institute, 4001 Miranda Avenue, Palo Alto, CA 94304, USA.

*To whom all correspondence should be addressed.

with EPO in receptor binding assays and induces cellular proliferation of cell lines engineered to be responsive to EPO. Both EPO and peptide induce a similar cascade of phosphorylation events and cell cycle progression in EPO responsive cells. Furthermore, EMP1 has significant erythropoietic effects in mice indicated by in vivo assays of nascent red blood cell production (*10*). These combined data support the conclusion that the peptide agonist, whose amino acid sequence is unrelated to that of EPO, can bind to and induce a biologically active conformation or assembly of EPOR.

Structural analysis of EPOR has been facilitated by the rapid growth of high-quality co-crystals of the EMP1 cyclic peptide and the extracellular ligand binding fragment (EBP) of EPOR. Our three-dimensional structure of the EBP-EMP1 complex provides new insights into (i) the fold and binding properties of the cytokine receptor superfamily, and (ii) the mechanism of activation of these receptors. Identification of the EPOR binding site may also provide valuable information toward optimization of the design and structure of a nonpeptide, small molecule EPOR agonist.

Structure of EBP-EMP1 complex. Human EBP, consisting of residues 1 to 225, was expressed in *Escherichia coli* and purified as described (*12*). Rhomboidal-shaped crystals of an EBP complex with EMP1 were obtained (*13*) in orthorhombic space group $P2_12_12_1$, with cell parameters a = 59.2 Å, b = 75.5 Å, c = 132.2 Å, with two EBPs (EBP1 and EBP2) and two peptide molecules in the asymmetric unit and a V_M = 2.8 Å^3/dalton (*14*). The crystal structure was determined by multiple isomorphous replacement (MIR) with two heavy-atom derivatives (Table 1 and Fig 1). Residues 1 to 2 and 19 to 20 of each peptide as well as residues 1 to 9, 21 to 23, 164 to 166, and 221 to 225 of EBP1, and residues 1 to 9, 21 to 23, 133 to 135, and 221 to 225 of EBP2 showed little or no electron density (*15*) and were excluded from the structure analyses.

The EBP monomer folds into two domains, D1 and D2, which form an L shape, with the long axis of each domain being aligned at approximately 90° to the other; the overall molecular dimensions are 45 by 68 by 24 Å^3 (Fig. 2A). The NH_2-terminal domain (D1, residues 10 to 114) and the COOH-terminal domain (D2, residues 119 to 220) are connected by a four-residue helical linker. Both domains are more closely related in overall topology to fibronectin type III (FBN III) domains than to Ig domains (*16*). The FBN III fold is composed of two antiparallel β-pleated sheets, consisting of strands A, B, and E and strands G, F, C, and C′; it is found in the two domains of the human growth hormone (*7*) and prolactin receptors (PRLR) (*17*), the D1 and D2 domains of the α chain of interferon-γ receptor (IFN-γRα) (*18*), the D2 domain of CD4 (*19*), the two domains of tissue factor (*20*), the third fibronectin-type repeat of tenascin (*21*), and the D2 domain of the chaperone protein PapD (*22*). Superposition of equivalent β-sheet core residues of the D1 and D2 domains in EBP gives a root-mean-square deviation (rms) of 2.3 Å for 77 Cα pairs, which is significantly larger than the corresponding domain overlaps for hGHbp (1.1 Å) and PRLR (0.8 Å), and reflects a difference in the subclass of fold between the two EBP domains.

In D1, a short α helix [residues 10 to 20; see (*15*)], precedes the first β sandwich that is better described as a hybrid of the FBN III fold with an Ig fold (residues 24 to 114), rather than strict FBN III topology. In this h-type fold (*16*), the C′ strand is long and

Table 1. Data collection and refinement statistics. Native crystallographic data were collected on a Siemens multiwire area detector mounted on a Elliott GX-18 generator, operating at 40 kV and 55 mA, with a crystal-to-detector distance of 120 mm. Two derivative data sets were collected on a MAR image plate mounted on a Siemens generator operating at 50 kV and 80 mA, with a crystal-to-image plate distance of 150 mm. Data were integrated, scaled, and reduced with the programs XENGEN (*51*) for the native data and DENZO and SCALEPACK (*52*) for the derivative data. Initial multiple isomorphous replacement anomalous scattering (MIRAS) phases were calculated to 3.1 Å by means of the program package PHASES (*53*) with a mean figure of merit of 0.64 (25.0 to 3.1 Å). Phases were refined in PHASES with the solvent flattening protocol to a mean figure of merit of 0.92 (25.0 to 3.1 Å). The quality of the map was generally good (Fig. 2), and 94 percent of the complex structure could be fitted with the use of the graphics program O (*54*). The register of the amino acid residues was verified from the positions of the two disulfide bridges in D1, and the positions of the two Hg's from the mercury acetate ($HgAc_2$) derivative, which were correctly assumed to bind to the free Cys^{181} residues. The peptide interpretation was verified from another data set from a complex between EBP and an iodinated peptide (Tyr^{P4} was substituted by *p*-iodo-Phe), which diffracted to 3.3 Å resolution, that in difference Fourier $(F_{iodo} - F_{nat})\alpha_{MIRAS}$ indicated the location of the iodine atoms (*55*). The structure was refined by means of the slow-cooling protocol in X-PLOR 3.1 (*56*) and rebuilt with $F_o - F_c$, $3F_o - 2F_c$ and SIGMAA weighted (*57*) electron density maps. After every two cycles of refinement, a set of simulated annealing omit maps (7 to 10 percent) to reduce model bias was calculated, and the entire structure was rebuilt. After several cycles of refinement, individual temperature factors were calculated and after ten cycles of refinement and model building, the R value was 0.21 for 8.0 to 2.8 Å data with $F > 1\sigma$ (13,984 reflections). The average thermal parameters for EBP1, EBP2, and the peptide dimer are 10.5, 12.3, and 10.7 Å^2, respectively. Only one nonglycine residue [Asn^{164} in EBP2], located in a weak electron density loop region in D2, is in a disallowed region in the Ramachandran plot. No solvent molecules were included in the model because of the moderate resolution (2.8 Å) of the structure determination. The coordinates have been deposited in the Protein Data Bank (*58*) and are on hold until 1 year from date of publication.

Data set	Resolution (Å)	Reflections (No.)	Completeness	R_{sym}*	Sites (No.)	R_{iso}†	R_{Cullis}‡	R_{Kraut}	Phasing power§	Resolution (Å)
Native	25.0–2.8	14158	0.93 (0.91)‖	0.05						
$HgAc_2$	25.0–3.0	11496	0.93 (0.91)	0.10	2	0.102	0.56	0.114¶	Iso 1.87	3.1
								0.100#	Ano 1.35	4.0
$UO_2(NO_3)_2$	25.0–3.0	11931	0.96 (0.94)	0.14	4	0.116	0.62	0.137¶	Iso 1.95	3.1
								0.114#	Ano 1.72	3.9

Refinement statistics:		Total number of atoms	R value (R_{free})	rms from ideal values		Average B value (Å^2)		
Resolution (Å)	Reflections $F > 1\sigma$			Bond length	Bond angle	EBP1	EBP2	Peptides
8.0–2.8	13894	3462	0.21 (0.34)	0.016 Å	2.1°	10.5	12.3	10.7

*$R_{sym} = \Sigma |I - \langle I \rangle| / \Sigma I$. Average I/σ for native data is 13.3 [2.7 in the outer shell (2.9–2.8 Å)]. †$R_{iso} = \Sigma |F_{PH} - F_P| / \Sigma F_P$. ‡$R_{Cullis} = \Sigma ||F_{PH} \pm F_P| - F_{H(calc)}| / \Sigma |F_{PH} - F_P|$ for all centric reflections. §Phasing power = $\{\Sigma |F_{PH(calc)}|^2 / \Sigma |F_{PH(obs)} - F_{P(calc)}|^2\}^{1/2}$; $|F_{PH(obs)} - F_{P(calc)}|$ is the lack of closure error to maximum resolution indicated. ‖Fractional completeness of data in the outer shell for the native (2.9–2.8 Å) and derivatives (3.1–3.0 Å). ¶$R_{Kraut} = \Sigma |F_{PH(obs)} - F_{PH(calc)}| / \Sigma F_{PH(obs)}$ for all acentric reflections (isomorphous case). #$R_{Kraut} = \Sigma ||F^+_{PH(obs)} - F^+_{PH(calc)}| + |F^-_{PH(obs)} - F^-_{PH(calc)}|| / \Sigma (F^+_{PH(obs)} + F^-_{PH(obs)})$ for all acentric reflections (anomalous case). Mean figure of merit = $<|\Sigma P(\alpha) e^{-i\alpha} / \Sigma P(\alpha)|>$ where $P(\alpha)$ is the phase probability.

interacts first with strand C and then switches to interact with strand E (where C′ changes its designation to strand D) forming a four-on-four strand β sandwich (Fig. 2B). D1 contains the two conserved disulfide bridges linking Cys^{28} (βA) to Cys^{38} (βB) and Cys^{67} (βC′) to Cys^{83} (βE). The number of residues between the cysteine pairs that form the two disulfide bridges are 9 and 15 for EBP, compared to 9 and 10 in both GHR and PRLR. The longer connection between strands C′ and E enables the second half of strand C′ to become strand D. This h-type topology is not found in either of the two s-type GHR domains. A potential glycosylation site exists on residue Asn^{52} which is located toward the end of the loop region connecting the βB and βC strands. Although Asn^{52} is not glycosylated in this bacterially expressed protein, an external cavity around the Asn^{52} side chain could easily accommodate a carbohydrate moiety (Fig. 2A).

A helical linker (residues 115 to 118) connects D1 to D2 (*23*) and has been observed in other family members, hGHbp, PRLR, IFN-γRα, and tissue factor. In EBP, the domain association is further restricted by a mixed assortment of hydrogen bonding, hydrophobic interactions, and one salt bridge (between Arg^{32} and Asp^{122}) from 11 residues of D1 and 12 residues of D2 with a total buried surface area (*24*) of 950 $Å^2$ for the two domains.

D2 (residues 119 to 220) folds into the standard FBN III (s-type) topology with one free cysteine and no disulfide bridges, consistent with GHR and PRLR that have three and two disulfide bridges, respectively, in D1 but none in D2. After the α helix linker, D2 begins with an irregular coil (residues 118 to 126) that contains Pro^{124}, which is structurally conserved in hGHbp, PRLR, tissue factor, and IFNγ-Rα, and, on the basis of sequence alignment, in most class-1 and class-2 cytokine receptors (*3*). This short coil ends with Gly^{126}, which has a positive ϕ (ϕ, ψ ≈ 52°, 40°) consistent with the equivalent Ala^{136} and Ala^{101} torsion angles in hGHbp (ϕ, ψ ≈ 63°, 68°) and PRLR (ϕ, ψ ≈ 58°, 38°). The Pro^{124} region forms an analogous extended bulge conformation adjacent and parallel to a corresponding bulge containing the WSXWS motif. The WSAWS sequence forms a modified wide β bulge (*25*) and is located in an extended chain region immediately preceding the βG strand that would normally connect to the membrane-spanning region of EPOR (Fig. 2A).

The quaternary structure of the complex is composed of two peptides and two receptors that form a T-shaped assembly. A noncovalent peptide dimer interacts with two receptor molecules to generate an almost perfect twofold symmetrical arrangement (Fig. 2A). After superposition of D2 of the two EBP molecules in the dimer, the centers of mass of the two D1 domains are only 0.8 Å apart, which is sufficient to perturb perfect twofold symmetry. Separate superposition of the corresponding D1 and D2 of each receptor in the dimer results in rms deviations of 0.53 Å (105 D1 Cα pairs) and 0.47 Å (93 D2 Cα pairs).

The cyclic EMP1 contains a single disulfide bridge between Cys^{P6} and Cys^{P15}, which links two short β strands (residues 4 to 7 and 13 to 16) that are connected by a slightly distorted type I β turn (*26*) consisting of residues Gly^{P9}–Pro^{P10}–Leu^{P11}–Thr^{P12}

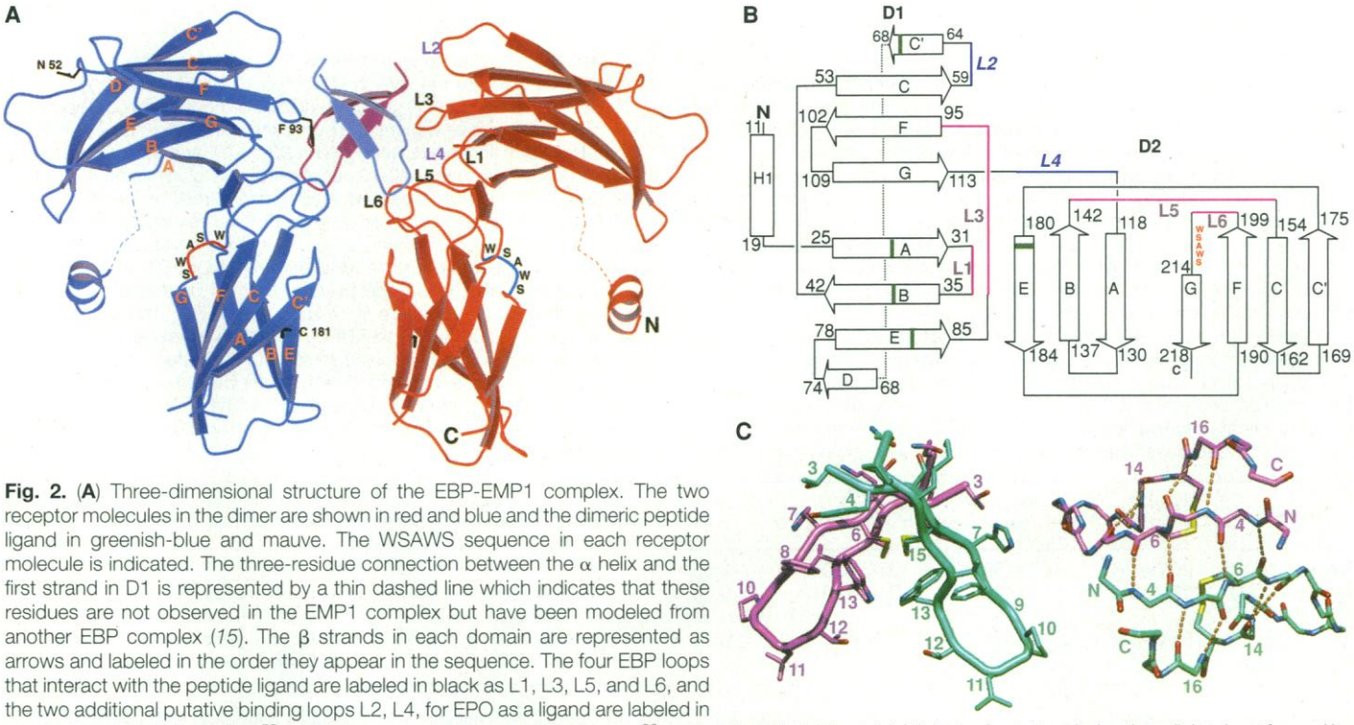

Fig. 2. (**A**) Three-dimensional structure of the EBP-EMP1 complex. The two receptor molecules in the dimer are shown in red and blue and the dimeric peptide ligand in greenish-blue and mauve. The WSAWS sequence in each receptor molecule is indicated. The three-residue connection between the α helix and the first strand in D1 is represented by a thin dashed line which indicates that these residues are not observed in the EMP1 complex but have been modeled from another EBP complex (*15*). The β strands in each domain are represented as arrows and labeled in the order they appear in the sequence. The four EBP loops that interact with the peptide ligand are labeled in black as L1, L3, L5, and L6, and the two additional putative binding loops L2, L4, for EPO as a ligand are labeled in purple. The side chains of Asn^{52}, which is a potential glycosylation site, Phe^{93}, which was found to be an essential side chain for high affinity EPO binding, and the free Cys^{181} are labeled in black. The figure was made with MOLSCRIPT (*49*). (**C**) The dimeric structure of the two EMP1 molecules as seen in the EBP-EMP1 complex. The left orientation shows the close association between the Trp^{P13} side chains from the two peptides (magenta and cyan), which are at the hydrophobic core of the peptide-peptide interface. Other consensus residues (*10*), Tyr^{P4}, Cys^{P6}, Cys^{P15}, in addition to Phe^{P8}, form hydrophobic interactions within the peptide dimer. The right view is rotated by 90° along the horizontal axis of the peptide backbone; all side chains are removed except for the disulfide bridge to highlight the four-stranded antiparallel β sheet formed by peptide-peptide dimerization. The two glycine residues (1 to 2, 19 to 20) at either termini are not observed in the electron density map, and the peptide shown consists of residues 3 to 18. (**B**) Topological diagram of the two domains of the EBP molecule. D1 consists of an h-type fold and D2 of an s-type fold (*16*). The positions of the five cysteine residues are marked in green bars. The four recognition loops of the EBP with the peptide ligand are drawn in pink and labeled L1, L3, L5, and L6; and the potential additional binding loops with its natural EPO ligand, based on the structures of hGH-hGHbp (*7*) and hGH-PRLR (*17*)complexes, are shown in blue and labeled L2 and L4.

(Fig. 2C). Each peptide has a very close association with its other peptide partner and buries 320 Å^2 of its 1220 Å^2 molecular surface in this interaction (*24*). Four hydrogen bonds between the main chains of the two peptides result in formation of a four-stranded, anti-parallel β-pleated sheet (Fig. 2C and Table 2). Two symmetric hydrophobic cores are assembled by peptide dimerization and are comprised of the disulfide bridges and the side chains of Tyr^{P4}, Phe^{P8}, and Trp^{P13}. The construction of each hydrophobic core resembles a box and places the aromatic rings of Phe^{P8}, Trp^{P13}, and Tyr$^{P'4}$, (from the other peptide) and the disulfide bridge (Cys^{P6}–Cys^{P15}) at the corners (Fig. 2C). The two glycine residues at either end of the peptide are not ordered.

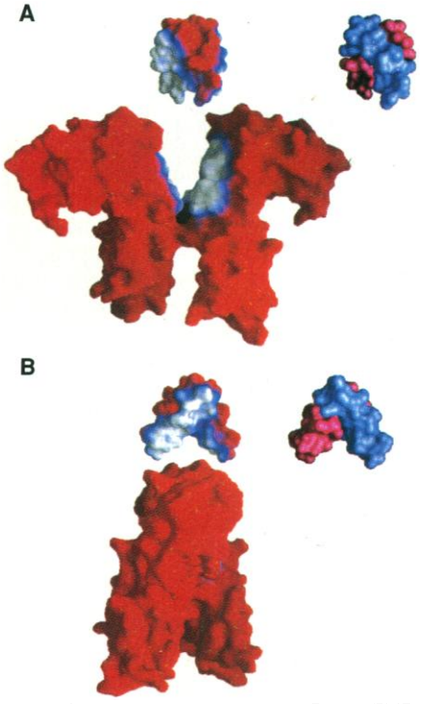

Fig. 3. Complementarity of the EBP and EMP1 surfaces in the complex. (**A**) A surface representation with GRASP (*50*) of each component is shown with the peptide dimer moved out from the binding site. The white surfaces represent contact areas on receptor and peptide dimer with surface-to-surface distances less than 2.5 Å. Blue and red colors represent distances of 2.5 to 5.0 Å and more than 5.0 Å, respectively. The peptide dimer fit tightly into the V-shaped binding site, which has relatively flat sides without any major cavities. The receptors are held together by interaction with the peptide dimer, since the receptor-receptor contact area (Leu^{175}, Arg^{178}) is negligible (75 Å^2) compared to each peptide-receptor binding site interaction (420 Å^2). An additional surface representation of the peptide dimer coloring the individual peptides in red and blue is shown on the upper right-hand side to emphasize the contribution of each peptide to the binding site of each receptor molecule. (**B**) a 90° rotated view along the vertical axis from (A).

The peptide dimer is embedded in a deep crevice between two EBP receptor molecules (Figs. 2A and 3). A portion of each peptide monomer interacts with both receptor molecules (Fig. 3). The binding sites of each EBP are practically identical as a result of the twofold symmetric interactions imposed on binding the peptide dimer. The four major contact areas on EBP come from segments on four loop regions (L1, L3, L5, and L6) that connect strands A to B (L1, residues 33 to 34) and E to F (L3, residues 90 to 94) in D1 and strands B to C (L5, residues 148 to 153) and F to G (L6, residues 203 to 205) in D2 (Figs. 2, A and B, and 4A). The areas of buried molecular surface (*24*) in the peptide-EBP assembly are 840 and 880 Å^2 for the two peptides and EBPs, respectively. The peptide-EBP interaction can be separated into distinct hydrophobic (67 percent) and polar (33 percent) areas. A hydrophobic core is formed between the peptide and receptor and comprises Phe^{93}, Met^{150}, and Phe^{205} from one EBP molecule and the peptide hydrophobic box consisting of Phe^{P8} and Trp^{P13} from one peptide and Tyr$^{P'4}$ and Cys$^{P'15}$ from the other peptide. The polar interactions are located chiefly at the bottom of the binding crevice and are mainly with loop L5 in D2. Five of the six hydrogen bonds are between the main chain of the β-turn residues Gly^{P9}, Pro^{P10}, and Leu^{P11} from one peptide with the main chain and side chains of residues in loop L5 of EBP. The other hydrogen bond is from the side chain hydroxyl of the consensus sequence Tyr$^{P'4}$, which crosses over its other peptide partner (Fig. 2C), to interact with loop L3 (Table 2). The EBP1-EBP2

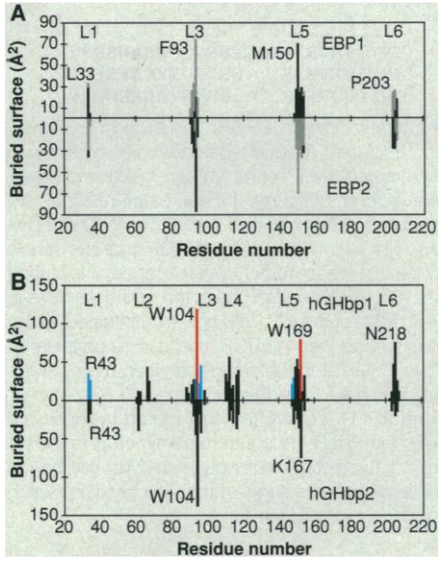

Fig. 4. Comparison of the binding determinants and buried surface areas (*24*) in the ligand-receptor interfaces of EBP-EMP1 and hGHbp-hGH; (**A**) Residues of EBP1 (top) and EBP-2 (bottom) that interact with the peptide dimer are distinguished by black and gray, respectively, to show the contribution of each peptide in the dimer to the buried surface of the receptor. Both peptides of the dimer contribute to each binding site such that the interface with EBP1, for example, consists mainly of residues from peptide 1 (L1, L5), peptide 2 (L3) or both (L6) and vice versa for EBP2. (**B**) Equivalent residues on the hGHbpI (top) and hGHbpII (bottom) that interact with hGH. The six interacting loops (L1 to L6) of hGHbp are shown in black with residues that contribute significantly to the binding energy (*43*) color-coded by red >4.5 kcal/mol and blue 1 to 3.5 kcal/mol. The EBP and the hGHbp were structurally aligned, so that the horizontal axis in hGHbp shows the EBP residue numbering.

Table 2. Hydrogen bond interactions in the binding site of the EBP-EMP1 complex. Because of the symmetrical nature of the complex, each binding site has equivalent interactions. The hydrogen bond interactions were based on both distance (3.9 Å cutoff) and geometrical considerations, with the use of HBPLUS (*59*).

Peptide-EBP	Peptide-peptide
Gly^{P9} O–Met^{150} N	Tyr^{P4}O–Cys^{P6}N
Pro^{P10} O–Thr^{151} N	Tyr^{P4}N–Cys^{P6}O
Pro^{P10} O–Thr^{151} Oγ	Cys^{P6}O–Tyr^{P4} N
Leu^{P11} O–Ser^{152} N	Cys^{P6}N–Tyr^{P4} O
Leu^{P11} O–Ser^{152} Oγ	
Tyr$^{P'4}$ OH–Ser^{92} N	

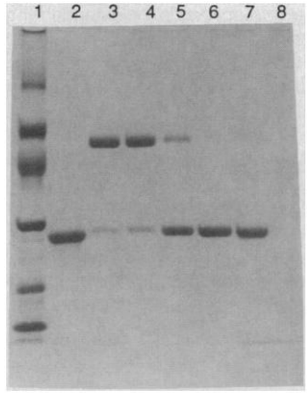

Fig. 5. Nonreducing SDS–polyacrylamide gel electrophoresis (SDS-PAGE) of DPDPB crosslinking of EBP in the presence and absence of EMP1. EBP and EMP1 were incubated together in the presence and absence of the homo-bifunctional sulfhydryl-reactive crosslinking reagent DPDPB in matched reagent mixtures. Only in the presence of crosslinker was formation of a higher molecular weight species observed. Lane 1, molecular markers; lane 2, 22 μM EBP; lanes 3 to 5, 400, 40, and 4 μM EMP1, respectively, with 22 μM EBP and 1.1 mM DPDPB, respectively; lane 6, no EMP1, 22 μM EBP, 1.1 mM DPDPB; lane 7, 400 μM EMP1, 22 μM EBP, no DPDPB; lane 8, 400 μM EMP1, no EBP, 1.1 mM DPDPB. The molecular mass of EBP is calculated at 24,724 daltons and the apparent dimer product appears between the 43- and 63-kD markers.

interaction contributes little to the overall stability of the complex where the buried molecular surface area between the receptors is only 75 Å^2 (Fig. 3A).

To explore the interaction of EMP1 with EBP in solution, we employed a bifunctional sulphydryl reactive crosslinker DPDPB (*27*), [1,4-di-(2′-pyridyldithio propionamido)butane]. A dimeric EBP product was formed only on co-incubation of EMP1, and EBP with DPDPB (Fig. 5). The crosslinked product was readily reversible by reduction (*28*). The two equivalent Cys^{181} residues in D2 of the EBP dimer are 20.7 Å apart [Sγ-Sγ distance], which approximates the 16 Å length [and approximately 2 Å bond length at each end] of the DPDPB crosslinker. Furthermore, we constructed a covalently linked dimeric form of EMP1 that had increased biological potency (*29*). Thus EMP1 mediates formation of a soluble EBP dimer complex in solution consistent with the crystal structure.

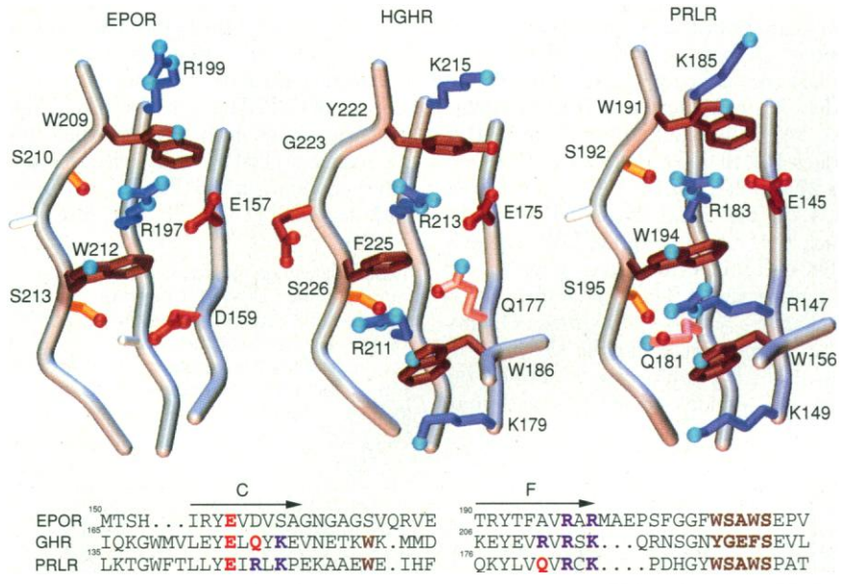

Fig. 6. Comparison of the WSXWS box and its structural vicinity in EPOR, GHR, and PRLR with corresponding sequence alignments. The side chains of different residue types are color-coded with aromatic (brown), positively charged (blue), negatively charged (red), serine (yellow), glutamine (pink), and alanine (white). In the receptor sequence alignment (bottom of figure), the equivalent residues are color-coded blue (positively charged), red (glutamic acid and glutamine) and brown (the WSXWS box and other tryptophans in the extended π-cation system). The π-cation system in EPOR consists of only one arginine and two tryptophan residues, which may explain the extremely low tolerance of mutating each of the tryptophans even to other aromatic residues (*37, 39*). Although one of the serine residues in replaced by a glycine in the HGHR, the structure of the β bulge of the WSXWS box is maintained. In the HGHR (*7*) and PRLR (*17*), the π-cation system is more extended than in EPOR, and can be considered as two subsystems with Phe^{225} in HGHR and Trp^{194} in PRLR at the interface between them. In the conserved π-cation system (top), the stacking of the conjugated residues are at ~4.0 Å spacings, whereas, in the additional π-cation system in GHR and PRLR (below), the conjugated residues are spaced ~3.6 Å apart. Additional Arg residues in HGHR and PRLR are contributed either from the βF strand as in hGHbp (Arg^{211}) or from βC as in PRLR (Arg^{147}); the glutamine residue that hydrogen bonds and orients the arginine also switches strands. Sequence alignments suggest that this Arg-Gln switch could be common to other members of the class-1 cytokine receptor family.

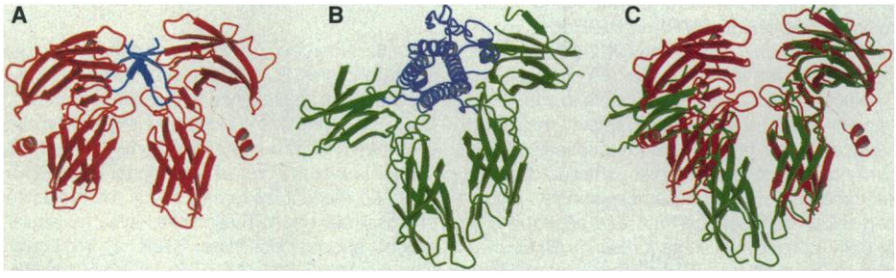

Fig. 7. Two biologically active dimeric arrangements seen in class 1 cytokine receptor complexes. (**A**) The individual EBP-EMP1 and (**B**) hGHbp-hGH complexes (*7*) are shown with their respective ligands in blue and receptor in red and green, respectively, to highlight the difference in size and shape of the peptide and hormone ligands that induce receptor dimerization. (**C**) EBP (red) and hGHbp (green) dimers superimposed only on one D2 from each dimer with the ligands omitted for clarity. This superposition illustrates not only the large difference in the dimer configuration between the two complexes, but also slightly different interdomain orientation in each receptor molecule. Two loop regions are missing in D1 of each hGHbp subunit (*7*) and one loop region in D2 of each EBP molecule (*45*).

EMP1 is one of a family of sequences that contain several conserved residues, besides the cysteines (*10*). EMP1 evolved from a peptide [AF11154; GGCRIGPITWVCGC] (*11*) that had low binding affinity (IC_{50} of approximately 10 μM) toward soluble EPOR (sEPOR) (*10*). This peptide already contained the sequence **GPXTW** which is involved both in peptide-receptor [Gly-Pro-X-Thr; type I β turn] and peptide-peptide [Trp] interactions (Fig. 2C). The next generation of peptides had a consensus sequence **YXCXXGPXTWXCXP**, which showed both increased binding (IC_{50} 0.2–1 μM) and biological activity. The introduced tyrosine side chain, along with the Trp, plays a key role in peptide-receptor interaction and dimerization (Table 2). In addition, the Tyr, Trp, and disulfide bridge make the major contribution to the hydrophobic core of the peptide dimer.

The WSXWS motif. The WSAWS sequence (residues 209 to 213) occurs in a β bulge (*25*) immediately preceding β strand G in D2 (Figs. 2A and 6) and adopts a polyproline type II helix conformation (*30*). This motif does not appear to play any role in ligand binding or receptor-receptor interaction (Fig. 2A). The WSAWS box represents only a segment of a complex array of interactions that includes several other conserved side chains from the four-stranded β sheet in D2 (Fig. 6). Ser^{210} and Ser^{213} form hydrogen bonds with the main chain of residues 198 and 196 of adjacent strand F in a pseudo–β-sheet type interaction that resembles a modified wide β bulge (*25*) where the side-chain hydroxyl rather than the carbonyl oxygen makes the β-sheet interaction. The polyproline type II architecture places the two Trp residues, which are three (*i*, *i* + *3*) residues apart, on the same side of the β sheet and not on opposite sides as in standard β-sheet or extended chain structures. The guanidinum group of Arg^{197} from strand F, the central residue (*25*) in the bulge, is positioned exactly between the two Trp indole rings to form an extended π-cation system (*31*). The three conjugated systems (*32*) are stacked parallel to each other, at approximately 4 Å spacings, such that the center of the pyrrole ring of Trp^{209}, the Nε of the Arg^{197}, and the center of the benzene ring of Trp^{212} are aligned. The side chain of

Glu[157] forms a hydrogen bond with Arg[197] and presumably influences the orientation of the guanidinium group. In addition, the aliphatic portion of the Arg[199] side chain makes hydrophobic contacts with the indole ring of Trp[209].

The structural equivalents of the WSXWS motif in hGHbp (YGEFS) and PRLR (WSAWS) take part in an even more intricate and complex array of π-cation interactions (Fig. 6). The extended π-cation system in hGHbp and PRLR consists of three aromatic groups that stack between five positively charged residues. The aliphatic portions of the outermost lysine side chains also form hydrophobic interactions with the aromatic rings (Fig. 6). A serine or threonine in positions 2 and 5 (*33*) maintain a common set of hydrogen bonds between their side chain hydroxyls and the main chain of the neighboring strand (Fig. 6). Sequence alignments and structural modeling (*34*) of other class-1 cytokine receptor superfamily members suggest that extended π-cation systems could exist in human thrombopoietin, IL-6, ciliary neurotrophic factor, and human IL-4 receptors (*35*).

Conservation of the WSXWS motif in EPOR or its equivalent in other members of the class-1 cytokine receptor family has been proposed to be essential for biological activity and was thus assumed to be part of the receptor binding site (*36*, *37*). For EPOR, a systematic study of 100 mutations of the WSAWS sequence demonstrates that most of the mutations of the two tryptophan and serine residues (*38*) resulted in molecules that did not reach the cell surface but were retained in the endoplasmic reticulum (*39*). Furthermore, an Ala[211] to Glu mutation resulted in better transportation from the ER to the Golgi and three to five times the number of EPOR molecules that reach the cell surface (*39*). These results now indicate a role for the WSXWS box in the folding and transport of receptor to the cell surface.

Comparison with other cytokine-receptor complex structures. The overall quaternary structure of the peptide-EBP complex differs from the equivalent arrangement in the hGH-hGHbp complex. The nonsymmetric nature of the single four-helix bundle structure of the growth hormone ligand results in an asymmetric homodimerization of the receptor that corresponds to a rotation of 159° between receptors compared to the almost perfect twofold (180°) rotation for the EBP-peptide complex (Fig. 7) (*40*). The tertiary arrangement of domains within EBP and hGHbp is also somewhat different. When the equivalent EBP and hGHbp D2 domains are superimposed on each other, their corresponding D1 domains differ by a 12° rotation and a 4.3 Å translation.

A sequential mechanism of hGH binding to its receptor has been well characterized (*6*). Initial high-affinity (nM) binding of the hormone with the first receptor hGHbp1 results in a buried surface area of 1130 Å^2 on the receptor. The second hGHbp2 has a substantially smaller interface (*7*) with the second binding site on hGH and interacts only with the preformed (1:1) complex to generate buried surface areas of 740 Å^2 with hGH and 440 Å^2 with the first hGHbp1 (*7*). The binding determinants of each hGHbp consist of six recognition loops (L1 to L6) (Fig. 4B), three of which (L1 to L3) come from one end of the β-sandwich structure in D1, one from the interdomain linker, and two from D2.

Although EBP-EMP1 and hGHbp-hGH complexes have different dimeric arrangements, which in this case probably represent differences in the size and shape of the natural hormone compared to the synthetic peptide, both receptors share equivalent ligand recognition loops, L1, L3, L5, and L6 for EBP and L1 to L6 for hGHbp (Fig. 4). A nonactive PRLR, complexed with only one molecule of hGH, also uses the same contact loops (L1 to L6) (*17*). From the similarity of the ligand recognition sites in hGHbp and PRLR, we would expect that the binding site of EBP, when its natural EPO ligand is bound, would include two additional loops, L2 and L4 (Fig. 2). These six loops in EBP, hGHbp, and PRLR are thus in structurally equivalent positions but vary in size, amino acid composition (*41*), and conformation, although the interacting portions of each loop (side or tip) remain similar; L1, L2, L3, and L5 interact mainly with their tips, and L6 interacts with its side. In one respect, this situation is similar to the complementarity-determining regions (CDRs) in antibodies, where changes in length and sequence of the six binding loops impose specificity for different antigens, but the framework itself remains constant (*42*).

For the hGHbp-hGH complex, only a subset of 9 out of 33 interacting residues that make up the structural epitope of the receptor constitute a "hot spot" or functional epitope (*43*), the site of high affinity binding interaction. This functional epitope is substantially smaller than the structural epitope and consists of residues Arg[43], Glu[44], Ile[103], Trp[104], Ile[105], Pro[106], Asp[165], and Trp[169], which are located in contact loops L1, L3, and L5 with the highest binding energy (>4.5 kcal/mol) coming from two aromatic residues (Trp[104] and Trp[169]) in L3 and L5 (Fig. 4) (*40*). In EBP, Phe[93] is equivalent to Trp[104] in hGHbp, as suggested (*43*, *44*), but there is no homologous residue to Trp[169] in the shorter L5 loop. In the EBP-EMP1 complex, the Phe[P8] peptide aromatic side chain occupies the equivalent position of the Trp[169] side chain in hGHbp. When EPO binds to its receptor, the hormone presumably may provide an aromatic residue to the hydrophobic core of the binding interface, or the L6 loop in EBP may play a more significant role in the hormone binding than in hGHbp because it is three residues longer and contains the aromatic Phe[205].

These three class-1 receptor structures all have some exposed loops that are disordered (*45*). Otherwise, these receptors have broadly similar tertiary structures such that the angle between the long axes of the D1 and D2 domains is approximately 90°. This arrangement of domains allows the loops L1 to L6 to be available for the recognition and binding of ligands (Fig. 2A) (*7*). In the IFN-γRα–IFN-γ complex, D1 and D2 are related by 125°, which restricts the binding determinants that are available for interaction with hormone; the L1 loop becomes buried in the D1-D2 interface, although the other five loops (L2 to L6) are still available for ligand interaction (*18*). This elongated interdomain arrangement is also observed in the blood coagulation tissue factor (*20*) which is a distant relative of the cytokine receptor superfamily.

A mutational analysis of the EBP molecule indicates that a crucial residue for binding EPO is Phe[93] in the L3 loop (*44*). The F93A mutant shows a decrease in binding to EPO as detected by an IC_{50} 1000 times higher than wild-type, whereas other mutants (S91A, S92A, V94A, M150A, and H153A) (*11*) have only small relative increases (2.5 to 12.5) in their IC_{50} (*44*). The side chain of Phe[93] buries 66 Å^2 of molecular surface, which is the highest among interacting side chains. In hGHbp, the corresponding W104A mutation results in a 2500 times increase in the K_d, indicating its key contribution to the hydrophobic core of the functional epitope (*43*, *46*).

Toward design of small molecule mimetics. In the EBP-EMP1 complex structure, we observe that a peptide, unrelated in sequence and probably in structure to the natural ligand, can induce a biologically active dimerization of EPO receptor that promotes signal transduction and cell proliferation. Comparison of three class-1 cytokine receptor complexes suggests that when the natural EPO hormone, which may have a structure of a four-helix bundle (*47*), induces receptor dimerization, it is more likely to resemble the hGH-hGHbp assemblage. More than one mode of productive extracellular dimerization may then be permissive for the intracellular dimerization of the cytoplasmic domains with two JAK2 molecules (*9*). The EBP-peptide structure

would represent only one possible dimeric arrangement that promotes signal transduction. Mutant EPOR molecules, containing a single Arg to Cys mutation (Arg^{130} in human and Arg^{129} in murine), form biologically active dimers in the absence of EPO (*48*), suggesting that extracellular receptor homodimerization may be sufficient in itself for signal transduction.

The structure of the EMP1 dimer demonstrates that a peptide considerably smaller than the natural hormone can act as an agonist and induce the appropriate biological response (*10*). The peptide can be assumed to form a substantially smaller contact interface with the receptor compared to the natural hormone. The peptide binding site in EBP forms an almost flat surface, which is mainly hydrophobic in nature, without any cavities or charged residues that are normally essential for the specific targeting of small molecule ligands to a receptor binding site. The hGHbp study (*43*) showed that only a small part of the observed structural binding site, the so-called functional epitope (*43*), contributes most of the binding energy and implied that a "minimized" hormone designed to interact with this site should form sufficient interactions to activate the receptor. Using a strategy designed initially to identify peptide binders from a phage display system (*10*), the EPO peptide mimetic surprisingly appears to have the characteristics of a minimal hormone. Furthermore, the limited site of interaction of the agonist peptide with EBP corresponds almost exactly to the smaller functional epitope derived from alanine scanning of hGH and hGHbp (*43*) (Fig. 4). Thus, by different means, we too have arrived at the conclusion that a small number of key interactions can contribute to a functional epitope on a receptor. Understanding of this simplified interaction surface can now be combined with further mutational and structural studies to assist in identifying the most crucial residues in the functional epitope, and consequently provide a practical target for drug design.

REFERENCES AND NOTES

1. S. B. Krantz, *Blood* **77**, 419 (1991); K. Jacobs *et al.*, *Nature* **313**, 806 (1985); L. O. Jacobson, E. Goldwasser, W. Fried, L. Pizak, *ibid.* **179**, 633 (1957).
2. P. Foa, *Acta Haematol.* **86**, 162 (1991); J. L. Spivak, Ed., *Erythropoietin: Basic and Clinical Aspects* (W. B. Saunders, Philadelphia, 1994), vol. 8, p. 863.
3. J. F. Bazan, *Proc. Natl. Acad. Sci. U.S.A.* **87**, 6934 (1990).
4. X is any amino acid residue.
5. C.-H. Heldin, *Cell* **80**, 213 (1995).
6. B. C. Cunningham *et al.*, *Science* **254**, 821 (1991); G. Fuh *et al.*, *ibid.* **256**, 1677 (1992).
7. A. M. de Vos, M. Ultsch, A. A. Kossiakoff, *ibid.* **255**, 306 (1992).
8. EPO binds two extracellular fragments of its receptor with affinities that differ by a factor of 1000. The reported K_d's for the first and second receptor molecules are of the order of nanomolar and micromolar, respectively [J. S. Philo *et al.*, *Biochemistry* **35**, 1681 (1996)].
9. J. N. Ihle, F. W. Quelle, O. Miura, *Seminars Immunol.* **5**, 375 (1993); U. Klingmüller, U. Lorenz, L. C. Cantley, B. G. Neel, H. F. Lodish, *Cell* **80**, 729 (1995).
10. N. C. Wrighton *et al.*, *Science* **273**, 458 (1996). The conserved residues in the family of EPOR binding peptides are Tyr^{P4}, Cys^{P6}, Gly^{P9}, Pro^{P10}, Thr^{P12}, Trp^{P13}, Cys^{P15}, Pro^{P17}. A sequence search in the SWISS-PROT database shows that the primary structure of EMP1 shares a high sequence identity to a family of bacterial peptides that go through post-translational modifications to become lantibiotics [J. N. Hansen, *Annu. Rev. Microbiol.* **47**, 535 (1993)].
11. Abbreviations for the amino acid residues are: A, Ala; C, Cys; D, Asp; E, Glu; F, Phe; G, Gly; H, His; I, Ile; K, Lys; L, Leu; M, Met; N, Asn; P, Pro; Q, Gln; R, Arg; S, Ser; T, Thr; V, Val; W, Trp; and Y, Tyr.
12. D. L. Johnson *et al.*, *Protein Express. Purif* **7**, 104 (1996).
13. E. A. Stura *et al.*, in preparation.
14. B. W. Matthews, *J. Mol. Biol.* **33**, 491 (1968).
15. An important break in the electron density that affects the structure interpretation occurs for the three residues (Arg^{21}-Gly^{22}-Pro^{23}) that link the NH_2-terminal α helix to the first β strand in D1 of both receptor molecules. A molecular packing diagram shows the proximity of a second noncrystallographically related dimer in the crystal that gives two possibilities of how this three-residue linker may be connected. Our choice of linker connectivity is based on a structure of another independent EBP-peptide complex at higher resolution (2.5 Å), which shares a similar molecular packing (O. Livnah *et al.*, unpublished data), but for which the electron density is clear for these three residues. At present we have not found any experimental data to verify whether this NH_2-terminal α helix exists in solution or is a crystallization packing artifact. This helical region is not observed in the known structures of hGHbp (begins at residue 32) (*7*), PRLR (begins at residue 2, without any defined secondary structure until the first β strand, residue 6) (*17*), the INF-γRα (begins at residue 17) (*18*), or tissue factor (begins at residue 3 without any defined secondary structure until the first β strand at residue 11) (*20*).
16. P. Bork, L. Holm, C. Sander, *J. Mol. Biol.* **242**, 309 (1994).
17. W. Somers, M. Ultsch, A. M. De Vos, A. A. Kossiakoff, *Nature* **372**, 478 (1994).
18. M. R. Walter *et al.*, *ibid.* **376**, 230 (1995).
19. J. H. Wang *et al.*, *ibid.* **348**, 411 (1990); S. E. Ryu *et al.*, *ibid.*, p. 419.
20. Y. A. Muller, M. H. Ultsch, R. F. Kelley, A. M. de Vos, *Biochemistry* **33**, 10864 (1994); K. Harlos *et al.*, *Nature* **370**, 662 (1994).
21. D. J. Leahy, W. A. Hendrickson, I. Aukhil, H. P. Erickson, *Science* **258**, 987 (1992).
22. A. Holmgren and C. I. Branden, *Nature* **342**, 248 (1989).
23. The φ, ψ torsion angles for the interdomain helical linker for Ile^{115}, Asn^{116}, Glu^{117}, and Val^{118} are −50°, −27°; −76°, −21°; −99°, 26°; and −151°, 38°, respectively.
24. The molecular surface areas buried by interaction were calculated with the use of the program MS [M. L. Connolly, *J. Appl. Crystallogr.* **16**, 439 (1983)] with a 1.74 Å probe sphere and standard atomic radii [D. R. Davies, E. A. Padlan, S. Sheriff, *Annu. Rev. Biochem.* **59**, 439 (1990)]. There may be some discrepancies between our values reported here and other (*7*) published values because we used a different algorithm [Connolly (above) compared to B. Lee and F. M. Richards, *J. Mol. Biol.* **55**, 379 (1971)] and different probe radii. For clarity, all values reported here have been calculated in the same way for better comparison between the receptors.
25. The bulge had been described as an irregular extended chain in the structures of hGHbp and PRLR (*7, 17*). We describe here this structural element as a modified wide β bulge [J. S. Richardson, *Adv. Prot. Chem.* **34**, 167 (1981); A. W. E. Chan, E. G. Hutchinson, D. Harris, J. M. Thornton, *Protein Sci.* **2**, 1574 (1993)] because of its shape, conformation, and pattern of hydrogen bond interactions with the adjacent β strand. Although there is no regular β structure immediately preceding or following the motif as is normally seen in standard β bulges, the adjacent pair of β strands (F and G) is in a conventional β sheet. The residue defined as X in a wide β bulge is Arg^{197} of strand F, and those as residues 1 and 2 are Ala^{211} and Trp^{212} of strand G, respectively.
26. Pro^{P10} (position $i + 1$) and Leu^{P11} ($i + 2$) of the β turn have φ, ψ = −62°, −38° and −99°, −60°, respectively. The carbonyl oxygen of Leu^{P11} has a hydrogen bond to EBP distorting the ψ value from its normal 0° ± 30° ($i + 2$) in a standard type I β turn.
27. The DPDPB crosslinker itself does not inactivate the EPO binding potential of EBP nor the proliferative properties of EMP1.
28. D. L. Johnson *et al.*, data not shown.
29. _____, in preparation.
30. The polyproline II left-handed helix is actually a common structural unit in globular proteins and has an average distribution of φ, ψ = −75°, 145° [A. A. Adzhubei and M. J. Sternberg, *J. Mol. Biol.* **229**, 472 (1993)]. Trp^{209}, Ser^{210}, Ala^{211}, Trp^{212} and Ser^{213} have φ, ψ = −68°, 142°; −75°, −174°; −80°, 162°; −80°, 162°; −70°, 167°, and −95°, 169°, respectively. The presence of a polyproline helical conformation in an FBN III domain was first noted in the structure of *Drosophila neuroglian* [A. H. Huber, Y. E. Wang, A. J. Bieber, P. J. Bjorkman, *Neuron* **12**, 717 (1994)].
31. R. A. Kumpf and D. A. Dougherty, *Science* **261**, 1708 (1993); D. A. Dougherty, *Science* **271**, 163 (1996).
32. The parallel stacking between the guanidinium group of arginine and aromatic rings is a common feature in protein structures [S. K. Burley and G. A. Petsko, *Adv. Prot. Chem.* **39**, 125 (1988); M. M. Flocco and S. L. Mowbray, *J. Mol. Biol.* **235**, 709 (1994)]; other observed cases of the rare triple parallel π stacking include Trp^{45}, Arg^{75}, and Tyr^{94} in tissue factor (*20*) and Phe^{201}, Arg^{203}, and Trp^{207} in leucine aminopeptidase [H. Kim and W. N. Lipscomb, *Biochemistry* **32**, 8465 (1993)], but these systems are not well aligned as in the cytokine receptor structures.
33. In hGHbp, there is no hydroxyl-containing residue at position 2, but Ser^{226} at position 5 still maintains an equivalent interaction.
34. A. Gustchina, A. Zdanov, C. Schalk-Hihi, A. Wlodawer, *Proteins* **21**, 140 (1995).
35. Although IFN-γRα and tissue factor do not have a WSXWS motif, the corresponding sequences TTEKS (residues 213 to 217) for IFN-γRα (*18*) and KSTDS (residues 201 to 205) for tissue factor (*20*), maintain a very similar β bulge.
36. A. Yoshimura *et al.*, *J. Biol. Chem.* **267**, 11619 (1992).
37. D. E. Quelle, F. W. Quelle, D. M. Wojchowski, *Mol. Cell. Biol.* **12**, 4553 (1992).
38. A Ser^{226} to Ala mutation also abrogates hGHR binding to hGH, and its expression on the cell surface is drastically reduced [J. W. Baumgartner, C. A. Wells, C. M. Chen, M. J. Waters, *J. Biol. Chem.* **269**, 29094 (1994)]. In GM-CSFRα and IL-2Rβ, point mutations of the serine residues cause a substantial decrease in cell surface expression but have little or no effect on ligand binding [L. V. Ronco *et al.*, *J. Biol. Chem.* **269**, 277 (1994); T. Miyazaki, M. Maruyama, G. Yamada, M. Hatakeyama, T. Taniguchi, *EMBO J.* **10**, 3191 (1991)].
39. D. J. Hilton, S. S. Watowich, P. J. Murray, H. F. Lodish, *Proc. Natl. Acad. Sci. U.S.A.* **92**, 190 (1995); D. J. Hilton, S. S. Watowich, L. Katz, H. F. Lodish, *J. Biol. Chem.* **271**, 4699 (1996).
40. Modeling and docking experiments of possible interactions between the two D2 domains of EBP did not provide a definitive answer as to how EBP1 and EBP2 might interact in the EPO-EBP complex.
41. In EBP, the L5 loop is three residues shorter than in hGHbp and PRLR, whereas the EBP L6 loop is three and four residues longer than in hGHbp and PRLR, respectively. The L2 loop also varies (six to ten residues) among the three receptors, but in EBP does not participate in peptide binding; in hGHbp, the L2 loop is partially disordered although it does contact the hormone.

42. I. A. Wilson *et al.*, in *Ciba Foundation Symp.* (Wiley, Chichester, 1991), vol. 159, p. 13.
43. J. A. Wells, *Curr. Opin. Cell Biol.* **6**, 163 (1994); T. Clackson and J. A. Wells, *Science* **267**, 383 (1995); J. A. Wells, *Proc. Natl. Acad. Sci. U.S.A.* **93**, 1 (1996).
44. L. K. Jolliffe *et al.*, *Nephrol. Dial. Trans.* **10**, suppl. 2, 28 (1995); S. A. Middleton *et al.*, *J. Biol. Chem.* **271**, 14045 (1996).
45. These correspond to residues 164 to 166 in EBP1 and 133 to 135 in EBP2, residues 55 to 58, 73 to 78 in hGHbp1, and 54 to 60, 73 to 75 for hGHbp2, and residues 31 to 33, 84 to 86 in PRLR.
46. S. H. Bass, M. G. Mullkerrin, J. A. Wells, *Proc. Natl. Acad. Sci. U.S.A.* **88**, 4498 (1991).
47. J.-P. Boissel, W.-R. Lee, S. R. Presnell, F. E. Cohen, H. F. Bunn, *J. Biol. Chem.* **268**, 15983 (1993).
48. S. S. Watowich *et al.*, *Proc. Natl. Acad. Sci. U.S.A.* **89**, 2140 (1992); S. S. Watowich, D. J. Hilton, H. F. Lodish, *Mol. Cell Biol.* **14**, 3535 (1994).
49. P. J. Kraulis, *J. Appl. Crystallogr.* **24**, 946 (1991).
50. A. Nichols, K. A. Sharp, B. Honig, *Proteins* **11**, 281 (1991).
51. A. J. Howard *et al.*, *J. Appl. Crystallogr.* **20**, 383 (1987).
52. Z. Otwinowski, in *Data Collection and Processing*, L. Sawyer, N. Isaacs, S. Bailey, Eds. (SERC Darsbury Laboratory, Warrington, 1993), pp. 56.
53. W. J. Furey, PHASES—A program package and analysis of diffraction data from macromolecules, (American Crystallographic Association Fourtieth Anniversary Meeting, New Orleans, 1990).
54. A. T. Jones, J. Y. Zou, S. W. Cowan, M. Kjeldgaard, *Acta Crystallogr.* **A47**, 110 (1991).
55. The data for the Tyr^{P4} substituted by a *p*-iodo-Phe are not shown.
56. A. T. Brünger, A. Krukowski, J. W. Erickson, *Acta Crystallogr.* **A46**, 585 (1990); A. T. Brünger, *X-PLOR, Version 3.1: A System for X-ray and NMR* (Yale Univ. Press, New Haven, 1992).
57. R. J. Read, *Acta Crystallogr.* **A42**, 140 (1986).
58. F. C. Bernstein *et al.*, *Arch. Biochem. Biophys.* **182**, 584 (1978).
59. I. K. McDonald and J. M. Thornton, *J. Mol. Biol.* **238**, 777 (1994).
60. We thank A. M. DeVos for hGH-PRLR coordinates, M. R. Walter for IFN-γRα-IFN-γ coordinates, M. Pique for help in preparing Fig. 6, E. Tsao and K. Frame for fermentations, F. McMahon for technical assistance, and K. Hoey for peptide synthesis. Supported in part by NIH grant GM-49497 (I.A.W.) and the Rueff-Wormser Scholarship Fund (O.L.). This is publication 9888-MB from the Scripps Research Institute. This article is dedicated to the memory of our colleague Jairo H. Arévalo.

18 March 1996; accepted 3 June 1996